ISSN 0021-8944, Journal of Applied Mechanics and Technical Physics, 2016, Vol. 57, No. 3, pp. 559–568. © Pleiades Publishing, Ltd., 2016.
Original Russian Text © V.P. Radchenko, M.N. Saushkin, V.V. Tsvetkov.

EFFECT OF THERMAL EXPOSURE ON THE RESIDUAL STRESS RELAXATION IN A HARDENED CYLINDRICAL SAMPLE UNDER CREEP CONDITIONS

V. P. Radchenko, M. N. Saushkin, and V. V. Tsvetkov

UDC 539.376:539.4.014.13

Abstract: This paper describes the effect of thermal exposure (high-temperature exposure) ($T = 675°C$) on the residual creep stress relaxation in a surface hardened solid cylindrical sample made of ZhS6UVI alloy. The analysis is carried out with the use of experimental data for residual stresses after micro-shot peening and exposures to temperatures equal to $T = 675°C$ during 50, 150, and 300 h. The paper presents the technique for solving the boundary-value creep problem for the hardened cylindrical sample with the initial stress–strain state under the condition of thermal exposure. The uniaxial experimental creep curves obtained under constant stresses of 500, 530, 570, and 600 MPa are used to construct the models describing the primary and secondary stages of creep. The calculated and experimental data for the longitudinal (axial) tensor components of residual stresses are compared, and their satisfactory agreement is determined.

Keywords: cylindrical sample, surface plastic hardening, micro-shot peening, residual stresses, temperature exposures, creep, rheological model, boundary-value problem, stress relaxation.

DOI: 10.1134/S0021894416030202

INTRODUCTION

In mechanical engineering, aerospace industry, and power industry, the operational characteristics of structural parts and elements are initially determined by the condition of the surface layer, especially compressive residual stresses arising in various technological treatment processes. Since the 1960's, the theoretical and experimental studies of the residual stress formation after the procedure of surface plastic hardening have been described in many works (see, e.g., [1–6]). The treatment of the material with the use of surface plastic deformation changes its structure and hardness, and the induction of compressive residual stresses improves the operational characteristics of the parts (fatigue resistance, corrosive cracking, tribological characteristics, etc.) at normal and moderate temperatures. This problem is also relevant in modern time. It was found in [7–17] that, for instance, the fatigue resistance of surface hardened parts is significantly affected by compressive residual stresses.

The feasibility of using surface plastic strain to increase the fatigue and long-term strength and so on under high temperatures is determined by the nature of the relaxation of induced compressive residual creep stresses under the condition of thermal exposure (temperature exposure without loading) and by the effect of quasistatic and cyclic loads. A large number of works devoted to the study of the residual stress relaxation under high-temperature loading are experimental. The relaxation of induced residual stresses in the simplest parts (cylindrical hollow and solid samples and prismatic bodies) under the condition of thermal exposure or uniaxial loading under high temperatures was studied in [18–25], and the effect of cyclic loads on the residual stress relaxation was touched upon in [26–29]. Radchenko et al. [30] carried out an experimental research of temperature exposures and multicyclic

Samara State Technical University, Samara 443100, Russia; radch@samgtu.ru; saushkin.mn@samgtu.ru; vi.v.tsvetkoff@mail.ru. Translated from Prikladnaya Mekhanika i Tekhnicheskaya Fizika, Vol. 57, No. 3, pp. 196–207, May–June, 2016. Original article submitted February 16, 2015.

fatigue tests on the physical and mechanical characteristics (mircohardness, surface roughness, and grain size) in hardened hollow cylindrical samples made of aluminum alloys.

The theoretical methods for estimating the residual stresses in the course of their formation after hardening and in the process of their relaxation are in the stage of development and mainly represent uniaxial (rod) models [19, 29]. The complete solution of the problem of the residual stress relaxation for a hardened cylindrical sample under tension due to creep is described in [6, 31], and the solution for the solid cylindrical sample under combined tension and torsion is given in [32]. However, the relationships describing the relaxation process were only validated for solid cylindrical samples under thermal exposure [31] with the use of the experimental data [2] for the axial component of residual stresses after hardening and thermal exposure. In [32], the creep model was constructed with the use of data from other papers for the reason that the experimental creep curves for the material under study were not presented in [2].

The goal of this paper is to theoretically study the effect of thermal exposure (high-temperature exposure) on the residual stress relaxation in a surface hardened solid cylindrical sample in order to test the adequacy of the method proposed in [31]. We used the experimental data [19] on the kinetics of residual stresses for a cylinder of ZhS6UVI alloy after micro-shot peening at room temperature ($T = 20°$C) at time $t = 0$ and after exposures at $T = 675°$C at times $t = 50$, 150, and 300 h. The experimental creep curves of the ZhS6UVI alloy at $T = 675°$C and under different stresses are also in [19].

The solution of the problem includes the following steps: (1) the formation of the initial stress–strain state in the sample after surface plastic strain by the technique described in [6, 33]; (2) the calculation of the residual stress fields in the hardened sample with temperature loading from $T = 20°$C (hardening temperature) to $T = 675°$C (thermal exposure temperature) ($t = 0$); (3) the solution based on the technology [31] for the boundary-value problem of residual stress relaxation under creep conditions with thermal exposure ($T = 675°$C); (4) the calculation of the final fields of residual stresses with temperature unloading from $T = 675°$C to $T = 20°$C for a predetermined time after completion of the creep process.

1. FORMATION OF THE INITIAL STRESS–STRAIN STATE IN A SOLID CYLINDRICAL SAMPLE AFTER SURFACE PLASTIC STRAIN

Let residual stresses and plastic strains be induced by means of surface plastic strain (air-shot peening) in the surface layer of the solid cylindrical sample of radius R. The problem is solved in a standard cylindrical coordinate system (r, θ, z). The radial, circumferential, and axial residual stresses are denoted by $\sigma_r^{\rm res}$, $\sigma_\theta^{\rm res}$, and $\sigma_z^{\rm res}$, and the corresponding tensor components of residual plastic strains after hardening are referred to as q_r, q_θ, and q_z. The off-diagonal components of the residual stress and plastic strain tensors are neglected due to their smallness as compared with diagonal components.

In the assumption that there are no secondary plastic strains in the compression region of the surface layer and with the use of the experimentally determined component $\sigma_\theta^{\rm res} = \sigma_\theta^{\rm res}(r)$, the following dependences were obtained for other components of residual stress and plastic strain tensors in [6, 33]:

$$\sigma_r^{\rm res} = -\frac{1}{r}\int\limits_r^R \sigma_\theta^{\rm res}(\xi)\,d\xi; \tag{1}$$

$$q_\theta(r) = \frac{(1+\mu)(1-2\mu)}{E(1+\alpha\mu)^2}\,r^{-\nu}\int\limits_0^r \xi^{\nu-1}\Big[\sigma_r^{\rm res}(\xi) + (1+\alpha)\sigma_\theta^{\rm res}(\xi)\Big]\,d\xi$$

$$-\frac{1+\mu}{E(1+\alpha\mu)}\Big[(1-\mu)\sigma_\theta^{\rm res}(r) - \mu\sigma_r^{\rm res}(r)\Big], \quad \nu = \frac{2+\alpha}{1+\alpha\mu}; \tag{2}$$

$$q_z(r) = \alpha q_\theta(r), \qquad q_r(r) = -(1+\alpha)q_\theta(r); \tag{3}$$

$$\varepsilon_z^0 = \frac{2}{R^2}\int\limits_0^R r\Big(q_z(r) - \frac{\mu}{E}\Big[\sigma_r^{\rm res}(r) + \sigma_\theta^{\rm res}(r)\Big]\Big)\,dr; \tag{4}$$

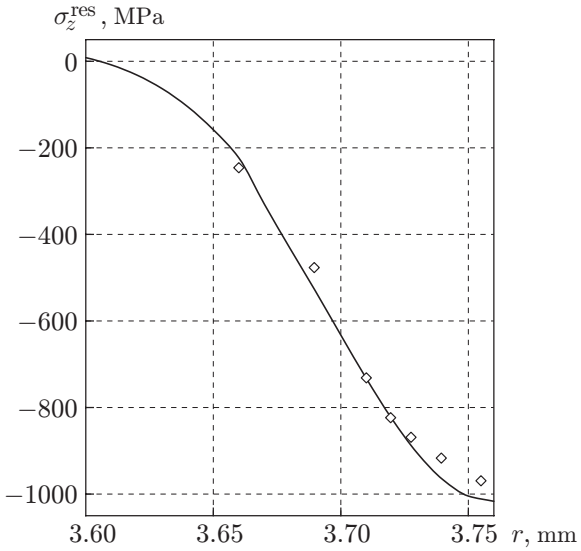

Fig. 1. Distribution of the axial component over the radius of the cylindrical sample made of ZhS6UVI alloy after hardening: curves denote calculations and points denote the experiment.

$$\sigma_z^{\rm res}(r) = E\Big(\varepsilon_z^0 - q(r)\Big) + \mu\Big(\sigma_r^{\rm res}(r) + \sigma_\theta^{\rm res}(r)\Big). \tag{5}$$

Here E is Young's modulus, μ is Poisson's ratio, and α is the phenomenological hardening anisotropy parameter [19, 22]. In the case of air-shot peening $\alpha = 1$, the stress diagrams $\sigma_\theta^{\rm res}$ and $\sigma_z^{\rm res}$ are practically identical [6].

The scheme for calculating the fields of residual stresses and plastic strains in the solid cylinder after hardening of its surface (at time $t = 0 - 0$) has the form

$$\sigma_\theta^{\rm res}(r) \xrightarrow{(1)} \sigma_r^{\rm res}(r) \xrightarrow{(2)} q_\theta(r) \xrightarrow{(3)} q_r(r), \quad q_z(r) \xrightarrow{(4)} \varepsilon_z^0 \xrightarrow{(5)} \sigma_z^{\rm res}(r) \tag{6}$$

(the numbers above the arrows indicate the numbers of expressions used to calculate the corresponding value). Scheme (6) shows that the components $\sigma_r^{\rm res}$, $\sigma_z^{\rm res}$, q_r, q_θ, and q_z are eventually determined via the parameter $\sigma_\theta^{\rm res}$ ($\alpha = 1$).

Thus, the phenomenological model (6) is based on the available experimental data about the distribution of the component $\sigma_\theta^{\rm res} = \sigma_\theta^{\rm res}(r)$. However, it can only be determined experimentally in a thin hardened layer (compression region), so these data are necessary to be extrapolated onto the entire region $0 \le r \le R$. For this purpose, we can use an approximation of the form

$$\sigma_\theta^{\rm res}(r) = \sigma_0 + \sigma_1\, {\rm e}^{-(R-r)^2/b^2}, \tag{7}$$

where σ_0, σ_1, and b are the approximation parameters [6].

Figure 1 shows the experimental and estimated values of the axial component $\sigma_z^{\rm res} = \sigma_z^{\rm res}(r)$ for the cylindrical sample of radius $R = 3.76$ mm made of ZhS6UVI alloy after the procedure of air-shot peening with $T = 20°$C, $E_0 = 2.3 \cdot 10^5$ MPa, and $\mu = 0.3$ [19]. Approximation (7) is constructed with the use of the self-equilibrium condition for the component $\sigma_\theta^{\rm res} = \sigma_\theta^{\rm res}(r)$:

$$\int_0^R \sigma_\theta^{\rm res}(r)\, dr = 0,$$

and also the conditions at the characteristic points

$$\sigma_\theta^{\rm res}(R) = \sigma^*, \qquad \sigma_\theta^{\rm res}(r_0) = 0, \tag{8}$$

where σ^* is the experimental value of the stress on the surface of the cylinder and r_0 is the radius at which the circumferential component is zero. These three conditions help us obtain a system of three nonlinear equations with respect to the parameters σ_0, σ_1, and b in Eq. (7), which is solved numerically. However, as the experimental

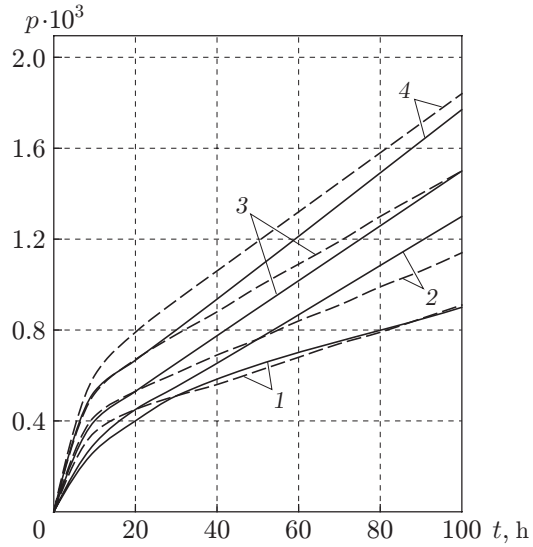

Fig. 2. Uniaxial creep curves for the ZhS6UVI alloy at $T = 675°$C and under different stresses: solid curves refer to the experimental data and dashed curves refer to the calculation by Eq. (11); $\sigma = 500$ (*1*), 530 (*2*), 570 ((*3*), and 600 MPa (*4*).

curve in [19] is shown for σ_z^{res} rather than for $\sigma_\theta^{\text{res}}$, the technique for determining the approximation parameters (7) becomes more complicated. Taking into account the similarity of the relationships $\sigma_\theta^{\text{res}} = \sigma_\theta^{\text{res}}(r)$ and $\sigma_z^{\text{res}} = \sigma_z^{\text{res}}(r)$, the initial approximations for σ^* and r_0 in Eqs. (8) are selected from the dependences for the axial component, the initial values of σ_0, σ_1, and b of approximation (7) are determined, scheme (6) is numerically implemented, the dependence $\sigma_z^{\text{res}} = \sigma_z^{\text{res}}(r)$ is determined, and the functional of the standard deviation of the calculated values of $\sigma_z^{\text{res}}(r_k)$ on the corresponding experimental values of $\sigma_z^{\text{res}*}(r_k)$:

$$\Delta_z(\sigma_0, \sigma_1, b) = \left(\sum_{k=1}^{N} \left[\sigma_z^{\text{res}}(r_k) - \sigma_z^{\text{res}*}(r_k) \right]^2 \Big/ \sum_{k=1}^{N} \left[\sigma_z^{\text{res}*}(r_k) \right]^2 \right)^{1/2} \tag{9}$$

(N is the number of sampling points of the radius r_k in the hardened layer).

Then, the problem is reduced to the optimization problem whose solution requires varying the variables σ^* and r_0 in Eqs. (8) and the parameters σ_0, σ_1, and b in Eq. (7); at the same time, scheme (6) is implemented on each step in order to reach the minimum value of the functional (9): $\Delta_z(\sigma_0, \sigma_1, b) \to \min$. The implementation of this scheme results in obtaining the following parameters: $\sigma_0 = 22.491$ MPa, $\sigma_1 = -1071.865$ MPa, and $b = 0.089$ mm. The deviation of the estimated values from the experimental values (see Fig. 1) is equal to $\Delta_z = 3.32\%$.

2. CONSTRUCTING THE CREEP MODEL OF THE ZHS6UVI ALLOY AT $T = 675°$C

One of the main stages in the solution of the problem of the residual stress relaxation is selecting a rheological model. Its construction requires the use of experimental creep curves for this alloy given in [19] (Fig. 2). There are two sections on these curves. Assuming that creep strain is irreversible, we use the creep model described by Samarin in [34], which has the following form in the case of uniaxial stress:

$$\begin{gathered} p = v + w, \qquad \dot{w}(t) = c\sigma^n, \qquad v(t) = \sum_{k=1}^{s} v_k(t), \\ \dot{v_k}(t) = \begin{cases} \lambda_k [a_k \sigma^m - v_k(t)], & a_k \sigma^m > v_k(t), \\ 0, & a_k \sigma^m \le v_k(t). \end{cases} \end{gathered} \tag{10}$$

Here v is the viscoplastic component of the creep strain p, w is the viscous flow strain, and c, n, λ_k, a_k, m, and s are the model parameters, whose determination technique is described in [34]. Under constant stress $\sigma = \text{const}$, expressions (10) for the creep curve help us obtain the dependence

$$p(t) = \sum_{k=1}^{s} a_k \Big(1 - \mathrm{e}^{-\lambda_k t}\Big)\sigma^m + c\sigma^n t. \tag{11}$$

Applying the procedure from [34] for the experimental data given in Fig. 2, we obtain the following approximation parameters (11) [consequently, models (10) too]: $s = 1$, $\lambda_k = \lambda = -0.21$, $m = 2.564$, $a_1 = a = 4.221 \cdot 10^{-11}$ MPa^{-m}, $n = 4.509$, and $c = 4.237 \cdot 10^{-18}$ MPa^{-n}. Figure 2 shows the approximating creep curves (11) as dashed curves. It can be seen that the calculated and experimental data are in good agreement. The deviation of the calculated values of the creep strain from the experimental values in the root-mean-square norm is found from the expression

$$\delta = \frac{1}{M}\sum_{i=1}^{M}\Big(\sum_{k=1}^{N}\Big[p_i(t_k) - p_i^*(t_k)\Big]^2 \Big/ \sum_{k=1}^{N}\Big[p_i^*(t_k)\Big]^2\Big)^{1/2}$$

and is equal to $\delta = 8.7\%$. Here M is the number of creep curves under constant stresses (in the present case, $M = 4$), N is the number of sampling points on each creep curve, t_k is the sampling time, and $p_i(t_k)$ and $p_i^*(t_k)$ are the calculated and experimental values of the creep strain, which correspond to the curve with the number i ($i = \overline{1, M}$).

For the case of a complex stress state, model (10) can be written in the form [34]

$$p_{ij} = v_{ij} + w_{ij}, \quad \dot w_{ij} = (3/2)cS^{n-1}(\sigma_{ij} - \sigma_0\delta_{ij}/3), \quad \sigma_0 = \sigma_{11} + \sigma_{22} + \sigma_{33},$$

$$\dot v_{\nu\nu}^k(t) = (1 + \mu_k)\beta_{\nu\nu}^k(t) - \mu_k(\beta_{11}^k(t) + \beta_{22}^k(t) + \beta_{33}^k(t)), \tag{12}$$

$$\dot\beta_{\nu\nu}^k = \begin{cases} \lambda[aS^{m-1}\sigma_{\nu\nu} - \beta_{\nu\nu}^k(t)], & aS^{m-1}\sigma_{\nu\nu} > \beta_{\nu\nu}^k(t), \\ 0, & aS^{m-1}\sigma_{\nu\nu} \le \beta_{\nu\nu}^k(t), \end{cases}$$

where p_{ij} is the creep strain tensor, w_{ij} and v_{ij} are the strain tensors of the viscous flow and viscoplastic (irreversible) component p_{ij}, S is the stress intensity, μ_k is Poisson's ratio for the component $v_{\nu\nu}$ (according to [34], $\mu_k = 0.42$), and c, n, λ, a, and m are the parameters having the same meaning as in approximation (11) with $s = 1$; the components v_{ij} are calculated in the main axes, so the summation for ν in expression (12) is not carried out.

3. SOLVING THE PROBLEM OF THE RESIDUAL STRESS RELAXATION IN THE HARDENED CYLINDRICAL SAMPLE DUE TO CREEP UNDER THE CONDITION OF THERMAL EXPOSURE WITH ACCOUNT FOR TEMPERATURE LOADING

We consider the temperature loading mode. Assuming that there are no additional plastic strains in the temperature loading of the sample from $T = 20°$C ($E_0 = 2.3 \cdot 10^5$ MPa) to $T = 675°$C ($E_1 = 1.85 \cdot 10^5$ MPa), expression (2) has the following form for the time of complete warm-up of the cylindrical sample (assuming it occurred instantly) at $T = 675°$C:

$$q_\theta(r) = \frac{(1+\mu)(1-2\mu)}{E_1(1+\alpha\mu)^2}\, r^{-\nu}\int_0^r \xi^{\nu-1}\,\frac{E_1}{E_0}\Big[\sigma_r^{\mathrm{res}}(\xi) + (1+\alpha)\sigma_\theta^{\mathrm{res}}(\xi)\Big]\,d\xi$$

$$- \frac{1+\mu}{E_1(1+\alpha\mu)}\,\frac{E_1}{E_0}\Big[(1-\mu)\sigma_\theta^{\mathrm{res}}(r) - \mu\sigma_r^{\mathrm{res}}(r)\Big], \quad \nu = \frac{2+\alpha}{1+\alpha\mu}; \tag{13}$$

because the value of $q_\theta(r)$ does not depend on temperature. Expression (13) is valid if, after hardening (with $E = E_0$), all the remaining residual stress diagrams are multiplied by the coefficient E_1/E_0 (so that we obtain the residual stress distribution at $T = 675°$C).

We consider the residual stress relaxation at $T = 675°$C due to creep strain. At $t = 0 + 0$ (after temperature loading up to $T = 675°$C), the stress–strain state of the cylindrical sample is determined by the residual stress tensor:

$$\sigma_{ij}(r, 0+0) = \begin{pmatrix} \sigma_r^{\mathrm{res}}(r) & 0 & 0 \\ 0 & \sigma_z^{\mathrm{res}}(r) & 0 \\ 0 & 0 & \sigma_\theta^{\mathrm{res}}(r) \end{pmatrix}. \tag{14}$$

The strain tensor components at any time t have the form

$$\varepsilon_r(r,t) = e_r(r,t) + q_r(r) + p_r(r,t), \quad \varepsilon_\theta(r,t) = e_\theta(r,t) + q_\theta(r) + p_\theta(r,t),$$
$$\varepsilon_z(r,t) = \varepsilon_z(t) = e_z(r,t) + q_z(r) + p_z(r,t), \tag{15}$$

where p_θ, p_z, and p_r are the creep strain tensor components; the elastic strains are determined from Hooke's law:

$$e_r(r,t) = [\sigma_r(r,t) - \mu(\sigma_\theta(r,t) + \sigma_z(r,t))]/E_1; \tag{16}$$

$$e_\theta(r,t) = [\sigma_\theta(r,t) - \mu(\sigma_r(r,t) + \sigma_z(r,t))]/E_1; \tag{17}$$

$$e_z(r,t) = [\sigma_z(r,t) - \mu(\sigma_\theta(r,t) + \sigma_r(r,t))]/E_1, \tag{18}$$

and, at $t = 0 + 0$, the stress tensor components are identical to the residual stress tensor components (14). In Eqs. (15), the temperature strains are not accounted for as they are uniform by the cylinder volume and do not affect the stress redistribution process due to creep; in addition, the plane section hypothesis is used $\varepsilon_z(r,t) = \varepsilon_z(t)$.

Substituting Eq. (18) in the third expression in system (15), we find

$$\sigma_z(r,t) = E_1\Big[\varepsilon_z(t) - q_z(r) - p_z(r,t)\Big] + \mu\Big[\sigma_\theta(r,t) + \sigma_r(r,t)\Big]. \tag{19}$$

Subtracting Eq. (17) from Eq. (16), we exclude the component $\sigma_z(r,t)$:

$$e_r(r,t) - e_\theta(r,t) = \frac{1+\mu}{E_1}\Big[\sigma_r(r,t) - \sigma_\theta(r,t)\Big]. \tag{20}$$

In view of the equilibrium equation

$$r\,\frac{d\sigma_r(r,t)}{dr} + \sigma_r(r,t) = \sigma_\theta(r,t), \tag{21}$$

Eq. (20) can be written in the form

$$e_r(r,t) - e_\theta(r,t) = -\frac{1+\mu}{E_1}\,r\,\frac{d\sigma_r(r,t)}{dr}. \tag{22}$$

We use the operator of the total derivative with respect to the variable r in Eqs. (21) and (22) and further for the stress tensor components and strain tensors as the time t is included in the expressions parametrically.

We differentiate expression (17) with respect to r:

$$\frac{de_\theta(r,t)}{dr} = \frac{1}{E_1}\Big[\frac{d\sigma_\theta(r,t)}{dr} - \mu\Big(\frac{d\sigma_r(r,t)}{dr} + \frac{d\sigma_z(r,t)}{dr}\Big)\Big]. \tag{23}$$

Differentiating Eq. (19) with respect to r and substituting $d\sigma_z/dr$ into Eq. (23), we find

$$\frac{de_\theta(r,t)}{dr} = \frac{1+\mu}{E_1}\Big[(1-\mu)\,\frac{d\sigma_\theta(r,t)}{dr} - \mu\,\frac{d\sigma_r(r,t)}{dr} + \frac{\mu E_1}{1+\mu}\Big(\frac{dq_z(r)}{dr} + \frac{dp_z(r,t)}{dr}\Big)\Big]. \tag{24}$$

After differentiating Eq. (21) with respect to r, expressing $d\sigma_\theta/dr$ from the resulting expression, and substituting it in Eq. (24), we have

$$\frac{de_\theta(r,t)}{dr} = \frac{1+\mu}{E_1}\Big[r(1-\mu)\,\frac{d^2\sigma_r(r,t)}{dr^2} + (2-3\mu)\,\frac{d\sigma_r(r,t)}{dr} + \frac{\mu E_1}{1+\mu}\Big(\frac{dq_z(r)}{dr} + \frac{dp_z(r,t)}{dr}\Big)\Big]. \tag{25}$$

Converting the strain compatibility equation

$$r\,\frac{d\varepsilon_\theta(r,t)}{dr} + \varepsilon_\theta(r,t) = \varepsilon_r(r,t)$$

and accounting for expressions (15) and (22), we obtain

$$r\,\frac{de_\theta(r,t)}{dr} = -\frac{1+\mu}{E_1}\,r\,\frac{d\sigma_r(r,t)}{dr} + (q_r(r) - q_\theta(r)) + (p_r(r,t) - p_\theta(r,t)) - r\Big(\frac{dq_\theta(r)}{dr} + \frac{dp_\theta(r,t)}{dr}\Big). \tag{26}$$

Substituting Eq. (25) into Eq. (26) and considering the expressions for plastic strains (3), we obtain the ordinary differential equation with respect to σ_r:

$$r^2\,\frac{d^2\sigma_r(r,t)}{dr^2}+3r\,\frac{d\sigma_r(r,t)}{dr}=g(r,t). \tag{27}$$

Here

$$g(r,t)=\frac{E_1}{1-\mu^2}\Big[\frac{2+\alpha}{1+\alpha}\,q_r(r)+p_r(r,t)-p_\theta(r,t)-r\Big(\frac{dp_\theta(r,t)}{dr}+\mu\,\frac{dp_z(r,t)}{dr}\Big)+\frac{r}{1+\alpha}\,(1+\mu)\,\frac{dq_r(r)}{dr}\Big]. \tag{28}$$

Equations (27) and (28) with the boundary conditions

$$\sigma_r(r,t)\Big|_{r=R}=0,\qquad \lim_{r\to 0}\frac{d\sigma_r}{dr}=0$$

constitute the boundary-value problem whose solution has the form

$$\sigma_r(r,t)=-\int\limits_r^R\frac{1}{\xi^3}\int\limits_0^\xi g(\eta,t)\eta\,d\eta\,d\xi. \tag{29}$$

Equation (29) describes the distribution of the radial stress tensor component σ_r.

The distribution of the circumferential component σ_θ can be found from the equilibrium equation (21) with known σ_r:

$$\sigma_\theta(r,t)=\frac{d}{dr}\,[r\sigma_r(r,t)]. \tag{30}$$

In order to determine σ_z using expression (19), we find the value of $\varepsilon_z(t)$ from the condition that the total thrust acting on the sample is zero:

$$\int\limits_0^R r\sigma_z(r,t)\,dr=0. \tag{31}$$

Substituting Eq. (19) into Eq. (31), performing the necessary operations of integration, and allowing the resulting relationship with respect to $\varepsilon_z(t)$, we obtain

$$\varepsilon_z(t)=\frac{2}{R^2}\int\limits_0^R r\Big(q_z(r)+p_z(r,t)-\frac{\mu}{E_1}\,[\sigma_r(r,t)+\sigma_\theta(r,t)]\Big)\,dr. \tag{32}$$

Calculating the value of $\varepsilon_z(t)$ in accordance with Eq. (32), we can find the function $\sigma_z(r,t)$ from Eq. (19).

Thus, we determine the kinetics of all stress tensor components in the surface layer with thermal exposure by using the algorithm

$$g(r,t)\xrightarrow{(28),(29)}\sigma_r(r,t)\xrightarrow{(30)}\sigma_\theta(r,t)\xrightarrow{(32)}\varepsilon_z(t)\xrightarrow{(19)}\sigma_z(r,t)$$

(the number above the arrows denote the number of the expression used to calculate the corresponding value).

Let the creep process be followed by the temperature unloading of the sample from $T=675^\circ$C ($E_1=1.85\cdot 10^5$ MPa) to $T=20^\circ$C ($E_0=2.3\cdot 10^5$ MPa) at $t=t^*+0$. As it is assumed that the plastic strains and accumulated creep strain components do not change during the temperature unloading, the residual stresses can be calculated at $t=t^*+0$ if the stress tensor components obtained by the time $t=t^*-0$ are multiplied by the coefficient E_0/E_1 (inverse to the coefficient with temperature loading).

4. NUMERICAL IMPLEMENTATION AND ANALYSIS OF THE RESULTS

In the implementation of the described technique, the problem was solved numerically using time steps. The rheological strain process was divided into segments $[t_j,t_{j+1}]$ of length Δt_j ($j=0,1,2,\ldots$), within in the limits of which the stress-state characteristics were assumed to be constant and corresponding to the time $t=t_j$ and the increments of the creep strain tensor components on this interval were calculated by the numerical integration of Eqs. (12) using Euler's method with $\sigma_{11}=\sigma_\theta$, $\sigma_{22}=\sigma_r$, and $\sigma_{33}=\sigma_z$. In the implementation of the proposed method, all of the derivatives were approximated by the corresponding difference relationships and the integrals were calculated by quadrature numerical integration formulas.

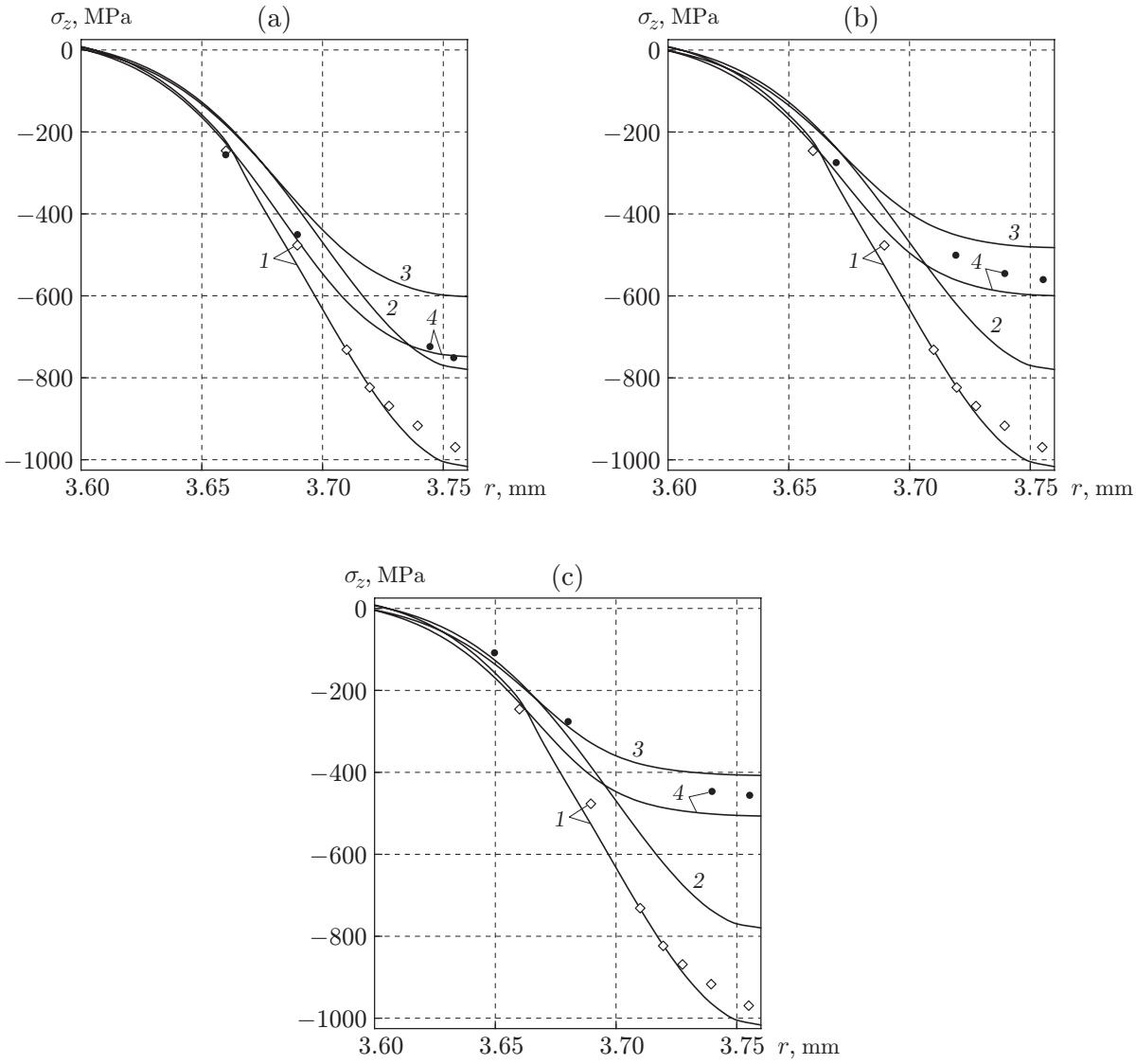

Fig. 3. Residual stress distribution σ_z in the cylindrical hardened sample over its radius at different times: (*1*) after hardening at $t = 0-0$; (*2*) after temperature loading from $T = 20°\text{C}$ to $T = 675°\text{C}$ at $t = 0+0$; (*3*) after the creep with thermal exposure at $T = 675°\text{C}$ and $t = 50-0$ (a), $150-0$ (b), and $300-0$ h (c); (*4*) final values after temperature unloading from $T = 675$ to $20°\text{C}$ at $t = 50+0$ (a), $150+0$ (b), and $300+0$ h (c); curves denote the calculation and points denote the experiment.

The calculation results of the residual stress relaxation $\sigma_z = \sigma_z(r,t)$ in the cylindrical hardened sample under the condition of thermal exposure at $T = 675°\text{C}$ and different exposure times are shown in Fig. 3. The points in Fig. 3 show the experimental data for the same strain component after micro-shot peening at $T = 20°\text{C}$ and the final data after the end of the creep process for the corresponding time and subsequent temperature unloading given in [19]. It can be seen that the calculated and experimental values of the component $\sigma_z = \sigma_z(r,t)$ are in satisfactory agreement. Note that the calculated and experimental data in the root-mean-square norm (9) differ by 3.32% after hardening; for the final stress diagrams, after the creep process of length $t = 50$, 150, and 300 h is completed and after subsequent temperature unloading, the difference in the values amounted to 2.85, 9.25, and 17.94%, respectively.

It follows from Fig. 3 that the maximum (in absolute value) calculated stresses σ_z in the relaxation process decreased by 22% for $t = 50$ h, by 39% for $t = 150$ h, and by 54% for $t = 300$ h; the experimental values decreased by 23, 42, and 57%, respectively.

Nevertheless, the residual stresses in the cylindrical sample made of ZhS6UVI are significantly high under the condition of thermal exposure during $t = (0–300)$ h at $T = 675°C$, which is very important because the efficiency of the use of the surface plastic strain methods (for example, to improve the fatigue resistance of parts in power engineering and aircraft engine manufacturing due to the presence of compressive residual stresses) is currently widely recognized [1–17, 19, 29, 31–33]. The values of the residual stresses in the creep process can help us judge upon the efficiency of the surface plastic strain methods (in the present case, air-shot peening) under the condition of the high-temperature loading.

This work was financially supported by the Ministry of Education and Science of the Russian Federation in the framework of the basic part of the state task of the Samara State Technical University (Grant No. 1151) and the Russian Foundation for Basic Research (Grant No. 16-01-00249).

REFERENCES

1. I. A. Birger, *Residual Stresses* (Mashgiz, Moscow, 1963) [in Russian].
2. V. F. Pavlov, V. A. Kirpichev, and V. B. Ivanova, *Residual Stresses and Fatigue Resistance of Reinforced Parts with Stress Concentrators* (Samara Scientific Center, Russian Acad. of Sci., Samara, 2008) [in Russian].
3. I. G. Grinchenko, *Reinforcement of Parts of Heat-Resistant And Titanium Alloys* (Mashinostroenie, Moscow, 1971) [in Russian].
4. B. A. Kravchenko, V. G. Krutsilo, and G. N. Gutman, *Thermoplastic Reinforcement—Strength and Reliability Enhancement for Machine Parts* (Samara State University, Samara, 2000) [in Russian].
5. A. M. Sulima, V. A. Shuvalov, and Yu. D. Yagodkin, *The Surface Layer and Performance of GTE* (Mashinostroenie, Moscow, 1988) [in Russian].
6. V. P. Radchenko and M. N. Saushkin, *Creep and Relaxation of Residual Stresses in Reinforced Structures*, (Mashinostroenie-1, Moscow, 2005) [in Russian].
7. I. Altenberger, R. K. Nalla, Y. Sano, et al., "On the Effect of Deep-Rolling and Laser-Peening on the Stress-Controlled Low- and High-Cycle Fatigue Behavior of Ti-6-Al-4V at Elevated Temperatures up to 550°C," Int. J. Fatigue **44**, 292–302 (2012).
8. R. A. Brockman, W. R. Braisted, S. E. Olson, et al., "Prediction and Characterization of Residual Stresses from Laser Shock Peening," Int. J. Fatigue **36** (1), 96–108 (2012).
9. K. Dai and L. Shaw, "Analysis of Fatigue Resistance Improvements via Surface Severe Plastic Deformation," Int. J. Fatigue **30** (8), 1398–1408 (2008).
10. M. N. James, D. J. Hughes, Z. Chen, et al., "Residual Stresses and Fatigue Performance," Eng. Failfure Anal. **14** (20), 384–395 (2007).
11. G. H. Majzoobi, K. Azadikhah, and J. Nemati, "The Effects of Deep Rolling and Shot Peening on Fretting Fatigue Resistance of Aluminum-7075-T6," Mater. Sci. Eng. **516** (1/2), 235–247 (2009).
12. R. C. McClung, "A Literature Survey on the Stability and Significance of Residual Stresses during Fatigue," Fatigue Fract. Eng. Mater. Struct. **30** (3), 173–205 (2007).
13. K. A. Soady, "Life Assessment Methodologies Incorporating Shot Peening Process Effects: Mechanistic Consideration of Residual Stresses and Strain Hardening. 1. Effect of Shot Peening on Fatigue Resistance," Mater. Sci. Technol. **29** (6), 637–651 (2013).
14. M. A. Terres, N. Laalai, and H. Sidhom, "Effect of Nitriding and Shot-Peening on the Fatigue Behavior of 42CrMo4 Steel: Experimental Analysis and Predictive Approach," Mater. Design **35**, 741–748 (2012).
15. V. F. Pavlov, "On the Relationship between the Residual Stress and Fatigue Strength at a Bend in the Conditions of Stress Concentration," Izv. Vyssh. Uchebn. Zaved., Mashinostroenie, No. 8, 29–32 (1986).
16. V. P. Radchenko and O. S. Afanas'eva, "Technique for Calculating the Fatigue Limit of Reinforced Cylindrical Samples with Stress Concentrators at Temperature Exposure," Vesnt. Samar. Gos. Tekh. Univ., Ser. Fiz.-Mat. Nauki, No. 2, 264–268 (2009).
17. V. F. Pavlov, V. A. Kirpichev, and V. S. Vakulyuk, *Prediction of Fatigue Strength of Surface Hardened Details Based on the Residual Stresses* (Izd. Samar. Nauch. Tsentra Ross. Akad. Nauk, Samara, 2012) [in Russian].
18. V. F. Pavlov, V. A. Kirpichev, and V. A. Lunin, "Impact on Thermal Exposition on Residual Stresses of the EP742 Sample Alloys after Ultrasonic Hardening," Vestn. Samar. Gos. Univ., Tekh. Univ., Ser. Tekh. Nauki, No. 3, 147–154 (2012).

19. V. I. Tseitlin and O. V. Kolotnikova, "Fatigue of Residual Stresses in the GTE Turbine Details in the Process of Operation," Probl. Prochnosti, No. 8, 982–984 (1980).
20. D. J. Buchanan and R. John, "Relaxation of Shot-Peened Residual Stresses under Creep Loading," Scripta Mater. **59** (3), 286–289 (2008).
21. Xie Lechun, Jiang Chuanhai, and Ji Vincent, "Thermal Relaxation of Residual Stresses in Shot Peened Surface Layer of (TiB+TiC)/Ti-6Al-4V Composite at Elevated Temperatures," Mater. Sci. Eng. A. **528** (21), 6478–6489 (2011).
22. B. J. Foss, S. Gray, M. C. Hardy, et al., "Analysis of Shot-Peening and Residual Stress Relaxation in the Nickel-Based Superalloy RR1000," Acta Mater. **61** (7), 2548–2559 (2013).
23. V. P. Radchenko, V. A. Kirpichev, and V. A. Lunin, "Impact of Air-Shot Peening and Thermal Exposition on Residual Stresses and Strength Limit of V95 and D16T Alloy Samples," Vestn. Samar. Gos. Tekh. Univ., Ser. Fiz.-Mat. Nauki, No. 3, 181–184 (2011).
24. J. Hoffmann, B. Scholtes, O. Vohringer, et al., "Thermal Relaxation of Shot Peening Residual Stresses in the Differently Heat Treated Plain Carbon Steel Ck 45," Shot Peening: Sci., Technol., Appl. **61** (7), 360–367 (1987).
25. M. Khadraoui, W. Cao, and L. Castex, "Experimental Investigations and Modelling of Relaxation Behaviour of Shot Peening Residual Stresses at High Temperature for Nickel Base Superalloys," Mater. Sci. Technol. **13** (4), 360–367 (1997).
26. A. Evans, S-B. Kim, J. Shackleton, et al., "Relaxation of Residual Stress in Shot Peened Idimet 720Li under High Temperature Isothermal Fatigue," Int. J. Fatigue. **27** (10), 1530–1534 (2005).
27. M. Benedetti, V. Fontanari, P. Scardi, et al., "Reverse Bending Fatigue of Shot Peened 7075-T651 Aluminium Alloy: The Role of Residual Stress Relaxation," Int. J. Fatigue **31** (8/9), 1225–1236 (2009).
28. Kim Jong-Cheon, Cheong Seong-Kyun, and Noguchi Hirochi, "Residual Stress Relaxation and Low- and High-Cycle Fatigue Behavior of Shot-Peened Medium-Carbon Steel," Int. J. Fatigue **56**, 114–122 (2013).
29. O. V. Kolotnikova, "Effectiveness of the Methods of Hardening by Surface Plastic Strain of Parts Operating at High Temperatures," Probl. Prochnosti, No. 2, 112–114 (1983).
30. V. P. Radchenko, A. P. Morozov, and V. A. Lunin, "Study on the Kinetics of Physical and Mechanical Parameters of B95 and D16T Alloys Due to Temperature Exposures and Multicycle Fatigue Tests," Vestnik. Samar. Gos. Tekh. Univ., Ser. Fiz.-Mat. Nauki, No. 1, 123–132 (2012).
31. V. P. Radchenko and M. N. Saushkin, "Direct Method of Solving the Boundary-Value Problem of Relaxation of Residual Stresses in a Hardened Cylindrical Specimen under Creep Conditions," Prikl. Mekh. Tekh. Fiz. **50** (6), 90–99 (2009) [J. Appl. Mech. Tech. Phys. **50** (6), 989–997 (2009)].
32. V. P. Radchenko and V. V. Tsvetkov, "The Kinetics of a stress–strain State in a Surface Hardened Cylindrical Sample in a Complex Stress State in Creep," Vestnik. Samar. Gos. Tekh. Univ., Ser. Fiz.-Mat. Nauki, No. 1, 93–108 (2014).
33. M. N. Saushkin, V. P. Radchenko, and V. F. Pavlov, "Method of Calculating the Fields of Residual Stresses and Plastic Strains in Cylindrical Specimens with Allowance for Surface Hardening Anisotropy," Prikl. Mekh. Tekh. Fiz. **52** (2), 173–182 (2011) [J. Appl. Mech. Tech. Phys. **52** (2), 303–310 (2011)].
34. Yu. P. Samarin, *Equation of State of Materials with Complicated Rheological Properties* (Kuybyshev State University, Kuybyshev, 1979) [in Russian].